Study of Confined 5-Aza[5]helicene in Ytterbium(III) Bis(2-ethylhexyl) Sulfosuccinate Reversed Micelles

Sergio Abbate,[†] Tullio Caronna,[‡] Alessandro Longo,[§] Angela Ruggirello,[▽] and Vincenzo Turco Liveri*[,▽]

Dipartimento di Scienze Biomediche e Biotecnologie, Università di Brescia, Viale Europa 11, 25123 Brescia, Italy, Dipartimento di Ingegneria Industriale, Università di Bergamo, Viale Marconi 5, 24044 Bergamo, Italy, ISMN, Istituto per lo Studio dei Materiali Nanostrutturati, Via U. La Malfa 153, 90146 Palermo, Italy, and Dipartimento di Chimica-Fisica "F. Accascina", Università degli Studi di Palermo, Viale delle Scienze Parco d'Orleans II, 90128 Palermo, Italy

Received: October 25, 2006; In Final Form: February 14, 2007

Some relevant physicochemical properties of 5-aza[5]helicene (H5) in solutions of ytterbium bis(2-ethylhexyl) sulfosuccinate ($Yb(DEHSS)_3$) reversed micelles have been investigated by UV−vis−NIR, photoluminescence, and FT-IR techniques with the aim of emphasizing the role played by specific Yb(III)/H5 interactions and confinement effects as driving forces of its binding to reversed micelles, preferential solubilization site, and local photophysical properties. It has been found that the binding strength of 5-aza[5]helicene to reversed micelles, triggered by steric and orientational constrains as well as the water content, is mainly regulated by its interaction with the Yb(III) counterion. Moreover, when H5 is entrapped in $Yb(DEHSS)_3$ reversed micelles, the combined action of this interaction and of confinement effects leads to marked changes of its photophysical properties with respect to those of H5 molecularly dispersed in apolar medium. The influence of the entrapment of finite amounts of H5 on the reversed micelle structure was investigated by SAXS. The analysis of experimental results brings to the hypothesis that H5 is preferentially solubilized and opportunely oriented in the micellar palisade layer and that its insertion causes an unidimensional growth of reversed micelles. From an analysis of WAXS spectra of H5/$Yb(DEHSS)_3$ composites, obtained by complete evaporation of the volatile components of the H5/water/$Yb(DEHSS)_3$/*n*-heptane solutions, it was ascertained that also on these systems H5 is dispersed molecularly or in a quite amorphous state in the surfactant liquid crystals without forming a separate crystalline nanophase.

Introduction

Sodium bis(2-ethylhexyl) sulfosuccinate (NaDEHSS) is a well-known surfactant widely employed to prepare solutions of reversed micelles in apolar media in a large composition range and without the need of cosurfactant agents. Thanks to their peculiar structure (a micellar core formed by the sodium counterions plus the hydrophilic heads of surfactant molecules and a surrounding hydrophobic layer composed by the opportunely arranged surfactant alkyl chains), reversed micelles show the remarkable ability to incorporate finite amounts of many ionic, polar, and amphiphilic substances. This fact opens the door to the study of some quite intriguing phenomena arising from the intramicellar confinement of these species, such as nanoparticles formation and local supersaturation effects.[1−3]

On the other hand, taking into account that the driving force of the solubilization process within NaDEHSS reversed micelles originates mainly from hydrogen bonding and dipolar interactions, it follows that such aggregates are unable to incorporate highly hydrophobic substances. In order to circumvent this problem and to extend confinement studies to some particularly interesting molecules, it has been suggested to use as surfactants some NaDEHSS derivatives ($M(DEHSS)_n$) obtained by simply replacing the sodium counterion with appropriately chosen M^{n+} cations that may establish sufficiently strong metal−ligand interactions with the selected species and enhance their entrapment into reversed micelles.[4] Depending on the nature of the counterion, this route could also confer tailored functionalities to the resulting micellar aggregates such as enhanced luminescence of the solubilized species, selective entrapment of hydrophobic substances, nanoparticle stabilization, and confinement of counterion−ligand complexes.[5−8]

Notwithstanding the large number of investigations concerning the solubilization within NaDEHSS reversed micelles, quite absent are specific studies of similar aggregates formed by $M(DEHSS)_n$. With the aim to gain some insight into this field, so as to exploit the peculiar subsequent physicochemical properties of helicenes in confined space, here we report the results of the successful attempt to confine 5-aza[5]helicene (H5) in reversed micelles formed by ytterbium(III) bis(2-ethylhexyl) sulfosuccinate ($Yb(DEHSS)_3$) in *n*-heptane.

5-Aza[5]helicene (the number in the square brackets indicates the number of aromatic rings in the molecule), whose structure is shown in Figure 1, is a representative component of a large class of screw-shaped molecules characterized by a chiral and delocalized π-electron system. Such structural peculiarities confer to these molecules the capability to self-assemble into columnar solid-state architectures and endows them with interesting optical and electronic properties, such as to make

* E-mail: turco@unipa.it. Tel.: +39 091 6459844. Fax: +39 091 590015.
[†] Università di Brescia.
[‡] Università di Bergamo.
[§] ISMN.
[▽] Università degli Studi di Palermo.

10.1021/jp066994i CCC: $37.00
Published on Web 04/04/2007

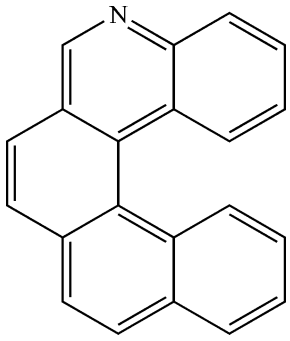

Figure 1. Molecular structure of 5-aza[5]helicene.

them a novel class of organic semiconductors. It has been suggested that possible applications of these compounds can be found in the fields of nonlinear optics and circularly polarized luminescence.[9,10] Moreover, association between helicenes and lanthanide ions shows the interesting property of harvesting UV−vis light and re-emitting it at a lower frequency whose value depends on the nature of the cation. This could allow the realization of tunable light emitters, photovoltaic cells, and low-frequency lasers. Among the various lanthanide ions as possible surfactant counterions, we have chosen ytterbium(III), since it shows an absorption band at about 980 nm, i.e., in a region quite free from other absorptions. This has allowed us to gain additional information on the Yb(III) ion environment.[11,12]

Since helicene molecules are chiral, one may envisage interesting applications that exploit such property. However in this work we have dealt with racemic mixtures of H5, and we defer the study of chirality in confined systems to future investigations.[13,14]

Experimental Section

Materials. Sodium bis(2-ethylhexyl) sulfosuccinate (NaDEHSS, Sigma 99%) was dried under vacuum for several days before use. *n*-Heptane (Aldrich, 99% spectrophotometric grade) and ytterbium(III) nitrate pentahydrate (Aldrich, 99.9%) were used as received. $Yb(DEHSS)_3$ was prepared by mixing appropriate amounts of an aqueous solution of $Yb(NO_3)_3$ with a 10^{-2} M aqueous solution of NaDEHSS. After aging, the precipitate was filtered, washed several times, and dried under vacuum for several days.[4] The synthesis and purification of 5-aza[5]helicene (H5, purity >99.99%) has been previously reported.[15]

Methods. $Yb(DEHSS)_3$/*n*-heptane solutions at various surfactant concentrations were prepared by weight, and the amount of water in these solutions, expressed as the molar ratio W (W = [water]/[$DEHSS^-$]), was determined spectrophotometrically by evaluating the intensity of the typical water band occurring at about 1920 nm.[16] To prepare samples in nearly anhydrous condition, solutions of $Yb(DEHSS)_3$ in *n*-heptane were stirred for 30 min in the presence of phosphorus pentoxide (Sigma, 99%) and then filtered. This procedure allowed us to reduce significantly the amount of water in the solutions without chemical modification of the surfactant.[17] H5-containing water/$Yb(DEHSS)_3$/*n*-heptane solutions at various H5 to $Yb(DEHSS)_3$ molar ratios R_{H5} (R_{H5} = [H5]/[$Yb(DEHSS)_3$]) were prepared by adding the appropriate amount of the water/$Yb(DEHSS)_3$/*n*-heptane solution to a weighted amount of H5. The solubility of H5 in pure solvents and in water/$Yb(DEHSS)_3$/*n*-heptane solutions at 25 °C was evaluated by inspection of samples at various H5 concentrations.

H5/$Yb(DEHSS)_3$ composites were prepared by evaporation of H5-containing water/$Yb(DEHSS)_3$/*n*-heptane solutions using a desiccator connected to a diaphragm vacuum pump (MZ2C, Vacuubrand).

UV−vis−NIR spectra were recorded in the wavelength range 200−2200 nm with a Perkin-Elmer (Lambda-900) spectrometer.

Photoluminescence spectra of samples excited with a laser source (Avalight-LED) at 380 nm were collected at room temperature in the range 300−1100 nm using an Avantes Avaspec-2048 spectrometer.

FT-IR spectra were recorded in the wavelength range 900−4000 cm^{-1} by a Perkin-Elmer (Spectrum BX) spectrometer using a fixed-path cell (about 0.1 mm) equipped with CaF_2 windows. All measurements were performed at 25 °C with a spectral resolution of 0.5 cm^{-1}.

Small-angle X-ray scattering (SAXS) patterns have been recorded by a laboratory instrumentation consisting of a Philips PW 1830 X-ray generator providing Cu Kα, Ni filtered (λ = 1.5418 Å) radiation with a Kratky small-angle camera in the "finite slit height" geometry equipped with step scanning motor and scintillation counter. Each scattering spectrum of freshly prepared samples was subtracted by the cell and solvent contributions. Best-fit analyses were performed by the CERN minimization program called MINUITS.

X-ray powder diffraction spectra of composites were performed by a Philips diffractometer (PW1050/39 X Change) equipped with a copper anode (Cu Kα, 1.5418 Å).

Results and Discussion

Preliminary experiments showed that the solubility (S) of H5 in water is lower than 10^{-5} M, while in pure *n*-heptane $S = 1.6 \times 10^{-3}$ M, and in a 0.066 M solution of NaDEHSS in *n*-heptane it increases up to $S = 6.4 \times 10^{-3}$ M. However, a more marked solubility increase is observed in the presence of $Yb(DEHSS)_3$. The solubility of H5 in a 0.068 M solution of $Yb(DEHSS)_3$ in *n*-heptane is S = 0.11 M at $W = 0.6$ and $S = 0.021$ M at $W = 2.0$ (W = [water]/[$DEHSS^-$]). These experimental results indicate that (i) $Yb(DEHSS)_3$ reversed micelles are particularly able to incorporate significant amounts of H5, (ii) Yb(III) plays a pivotal role in the binding process, and (iii) the solubilization ability of $Yb(DEHSS)_3$ reversed micelles is drastically influenced even by small amount of water.

Then, to achieve photophysical and structural information on the state of finite amounts of H5 confined in $Yb(DEHSS)_3$ reversed micelles, UV−vis−NIR, photoluminescence, FT-IR, and SAXS investigations on the prepared micellar systems for selected composition have been carried out. Moreover, taking into account the theoretical and technological importance of solubilizate/surfactant nanocomposites, preliminary structural information on some H5/$Yb(DEHSS)_3$ solid samples were also achieved by wide-angle X-ray scattering (WAXS).[18]

UV−Vis−NIR Spectra. Two representative UV−vis−NIR spectra of H5/water/$Yb(DEHSS)_3$/*n*-heptane solutions, from which the solvent contribution had been subtracted, are shown in Figure 2. For comparison, the solvent subtracted spectrum of the H5/*n*-heptane solution at the same H5 concentration is also shown. It can be noted that bands, marked by arrows, occur in the 240−400 nm range due to single-electron transitions between several H5 molecular orbitals,[19] at about 975 nm arising from the electric-dipole forbidden and magnetic-dipole allowed intraconfigurational transition $^2F_{7/2} \rightarrow {}^2F_{5/2}$ of Yb^{3+},[20,21] and at about 1920 nm due to the (1,1) combination mode of stretching and bending vibrations of water.[16,22] This latter band is a quantitative indicator of the amount of water encapsulated in the micellar core. In particular, a linear relationship between the water content and the absorbance at the band maximum has

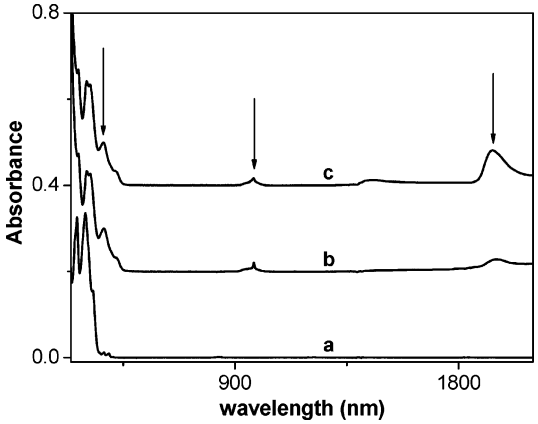

Figure 2. UV−vis−NIR spectra of (a) H5/*n*-heptane, (b) H5/water/Yb(DEHSS)$_3$/*n*-heptane ($W = 0.6$), and (c) H5/water/Yb(DEHSS)$_3$/*n*-heptane ($W = 2.0$) at fixed H5 and Yb(DEHSS)$_3$ concentrations ([H5] $= 1.23 \times 10^{-4}$ M, [Yb(DEHSS)$_3$] $= 0.068$ M).

been found allowing us to check the amount of water in all the investigated samples.[23]

Concerning the band due to H5, it is worth noting that the absorption onset, occurring at about 400 nm in the case of H5 in pure *n*-heptane and corresponding to the singlet−singlet $S_0 \rightarrow S_1$ 0−0 transition, is shifted at longer wavelength in the presence of the surfactant (about 470 nm).[15] This effect, caused by the decrease of the HOMO−LUMO energy gap, can be taken as an indication of the perturbation of the external H5 molecular orbitals induced by its binding with Yb(III).

The [Yb(DEHSS)$_3$] dependence of the H5 band shape at $W = 0.6$ and 2.0 is shown in Figure 3. Interestingly, the analysis of the spectra at $W = 0.6$ allows one to emphasize that, even at the lowest investigated surfactant concentration (0.0007 M), the H5 band is markedly different from that of H5 in pure *n*-heptane and it does not show significant changes by increasing [Yb(DEHSS)$_3$]. On the other hand at $W = 2.0$, after an initial progressive variation of the band shape, it does not vary significantly at [Yb(DEHSS)$_3$] ≥ 0.03 M. This behavior suggests that the H5/Yb(III) interaction is mediated by the water content, i.e., water competes effectively with H5 as ligand of Yb(III), thereby reducing its binding strength to reversed micelles. In particular at $W = 0.6$, independently on the surfactant concentration, H5 is practically totally confined in the reversed micelles; while at $W = 2.0$ it is partitioned between the *n*-heptane and the micellar phase. In order to test this hypothesis, we have attempted to obtain each spectrum as the linear combination of those of H5 in pure *n*-heptane and in Yb(DEHSS)$_3$/*n*-heptane solution at the highest investigated surfactant concentration (0.068 M), according to the equation

$$I_{(\nu)} = X_m I_{(\nu,\text{bonded})} + (1 - X_m) I_{(\nu,\text{free})} \quad (1)$$

where $I_{(\nu)}$ is the absorbance at the frequency ν, X_m is the fraction of H5 confined in the reversed micelles, $I_{(\nu,\text{bonded})}$ is the absorbance of H5 at the highest surfactant concentration investigated (0.068 M), and $I_{(\nu,\text{free})}$ that of H5 in pure *n*-heptane. It was found that all the spectra of Figure 3 can be satisfactorily described by eq 1 through the X_m value as single-fitting parameter. The dependence of X_m on the surfactant concentration is shown in Figure 4. It can be noted that, in addition to the previously emphasized features, X_m shows at $W = 2.0$ a peculiar trend which, on the basis of our present knowledge, we are unable to rationalize.

In order to obtain additional information on water/Yb(III) and H5/Yb(III) interactions we have also analyzed the Yb(III) NIR band. This band is characterized by a main peak occurring at about 975 nm accompanied by a side band due to lower energy transitions originated from excited thermally populated sublevels of the fundamental $^2F_{7/2}$ state.[21] As it is shown in Figure 5, shape, position, and intensity of the band are in fact perturbed by a change of the amount of water surrounding the Yb(III) ion. In particular, the wavelength (λ_{max}) and the molar extinction coefficient (ϵ_{max}) at the band maximum of Yb(III) in reversed micelles are higher than in pure water ($\lambda_{max} = 972$ nm, $\epsilon_{max} = 1.94$ M^{-1} cm^{-1}).[24] On the other hand, by increasing the molar ratio R_{H5} ($R_{H5} = [H5]/[Yb(DEHSS)_3]$) at fixed W, no significant change of the λ_{max} and ϵ_{max} is observed. This conclusion can be drawn from an analysis of the spectra of Figure 6 after appropriate subtraction of the tail of the H5 band occurring at higher frequencies. It is consistent with the hypothesis that the H5/Yb(III) interaction is weaker than the water/Yb(III) one. Incidentally it is worth to note that, by increasing R_{H5} at fixed surfactant concentration, the absorption onset of the band due to H5 is progressively shifted at longer wavelength reaching the NIR range at the higher R_{H5} values investigated.

Photoluminescence Spectra. The total photoluminescence of H5 can be ascribed to the radiative decay of both excited singlet (lifetime 3.5 ns) and triplet state which is populated by intersystem crossing (ISC) and characterized by fast ISC rate (KISC $\sim 10^7$ s^{-1}) and long lifetime (2.4 s).[15] These characteristics make H5 and its association with lanthanides a good choice for photo- and optoelectronic applications.

The [Yb(DEHSS)$_3$] dependence of the H5 photoluminescence spectra at $W = 0.6$ and 2.0 is shown in Figure 7. It can be noted that, at fixed H5 concentration ([H5] $= 1.23 \times 10^{-4}$ M), the presence of the surfactant induces a significant red shift of the band accompanied by a parallel pronounced increase of the H5 photoluminescence intensity with respect to that of H5 in pure *n*-heptane. Moreover, this effect appears to be more marked at the lower W value. It confirms the occurrence of interaction between H5 and Yb(III) and that this interaction is triggered by the water content, i.e., water competes with H5 effectively as ligand for Yb(III). In particular, the enhancement of the H5 photoluminescence can be attributed to the confinement within the Yb(DEHSS)$_3$ reversed micelles providing protection against deactivating interactions (excimer formation, triplet−triplet annihilation and quenchers), while the red shift can be caused by the stabilization of the H5 excited state due to its binding to Yb(III). The mechanism by which this stabilization is reached could be similar to that proposed by Horrocks et al.[25] involving the temporary transfer of an electron from the excited singlet state of H5 to the Yb(III) ion and the formation of Yb(II) and H5 cationic species. By back transfer of the electron to H5, excited Yb(III) and H5 at lower energy from the beginning will be then formed.

The pivotal role of Yb(III) counterion is also emphasized by the fact the H5 association with NaDEHSS reversed micelles does not display enhancement effects of its photoluminescence. In broad terms the confinement of H5 into Yb(DEHSS)$_3$ reversed micelles is seen to provide a nanocavity giving rise to a strong enhancement of photon emission, whereas too much water present in the micelle acts as a quencher of the process.

FT-IR Spectra. IR spectroscopy was chosen as a suitable technique to investigate the H5/water/Yb(DEHSS)$_3$/*n*-heptane system because it allows one to monitor phenomena on a time scale of about 10^{-13} s (shorter than most exchange processes occurring in the liquid phase), and therefore it allows one to achieve simultaneously detailed information on the state and environment of several molecular groups of interest through an

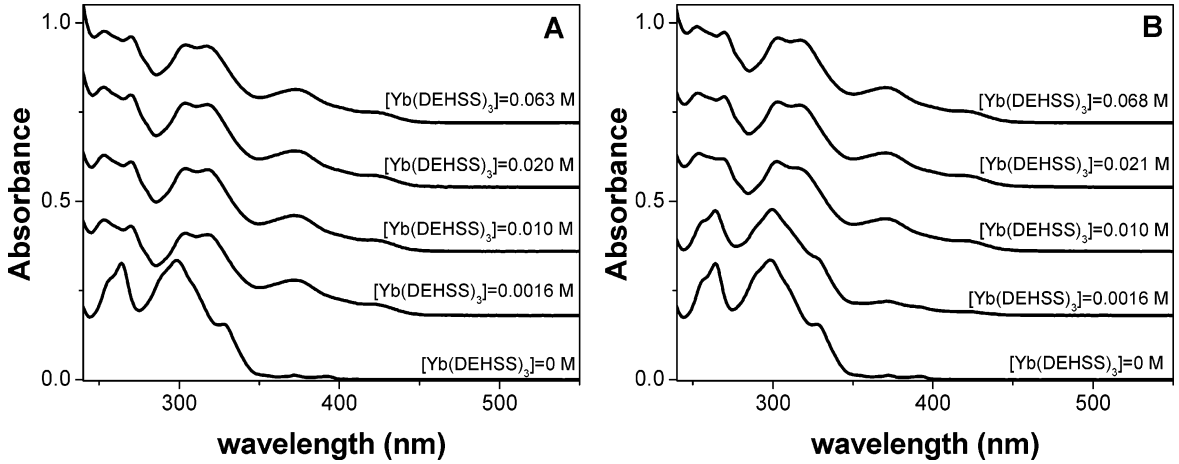

Figure 3. UV band of H5 in water/Yb(DEHSS)$_3$/*n*-heptane solutions as a function of surfactant concentration and fixed H5 concentration ([H5] $= 1.23 \times 10^{-4}$ M). Panel A, $W = 0.6$; panel B, $W = 2.0$.

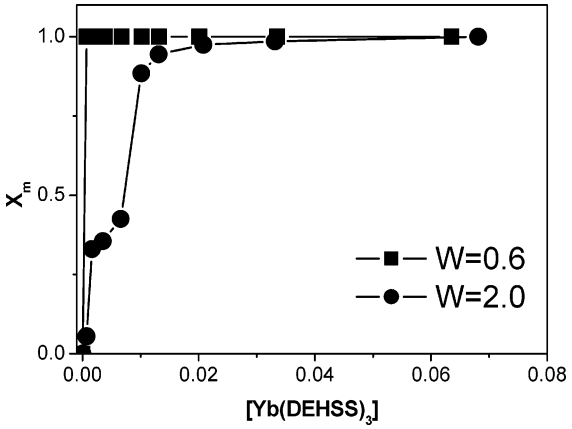

Figure 4. Fraction (X_m) of H5 confined in the reversed micelles as a function of the surfactant concentration at W shown and fixed H5 concentration ([H5] $= 1.23 \times 10^{-4}$ M).

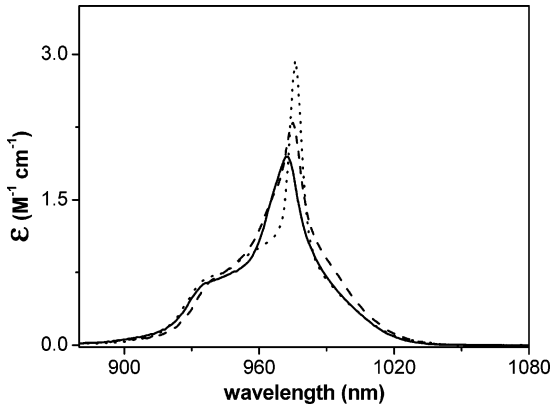

Figure 5. Absorption band of Yb(III) in Yb(DEHSS)$_3$/H_2O ([Yb(DEHSS)$_3$] = 0.0905 M, continuous line), water/Yb(DEHSS)$_3$/*n*-heptane ([Yb(DEHSS)$_3$] = 0.068 M, $W = 0.6$, dotted line), water/Yb(DEHSS)$_3$/*n*-heptane ([Yb(DEHSS)$_3$] = 0.068 M, $W = 2.0$, dashed line) systems.

analysis of their band shape and position.[17] The most significant features, which are analyzed here, are the stretching bands of water OH bonds, surfactant CO and SO_3^- groups, H5, CH, and CN groups.

The comparison of the water OH stretching band in water/Yb(DEHSS)$_3$/*n*-heptane system at $W = 0.3$ and 2.0 with the corresponding band in pure H_2O is shown in Figure 8. It can be noted that the position and shape of the OH band in water/Yb(DEHSS)$_3$/*n*-heptane solutions depends on the W value, and it is quite different from that of pure water. In particular, it is worth to note the increase of the contribution of the lower frequency components in the sample at $W = 0.3$ with respect to pure water. Taking into account that the water OH band in water/NaDEHSS/*n*-heptane solution at $W = 1.0$ is centered at about 3500 cm^{-1}, these effects consistently emphasize that water molecules are preferentially engaged in the coordination shell of the Yb^{3+} ions.[26] On the other hand, by adding H5 to the micellar solutions up to the R_{H5} value of 1.59, no significant effect on the OH stretching band is observed. This indicates that H5 is not able to displace effectively water from the solvation shell of Yb(III), i.e., the binding of H5 to Yb(III) is weaker than that of water.

Concerning the band at about 1740 cm^{-1} shown in Figure 9 A,B, assigned to the surfactant headgroup CO stretching, it can be noted that its position and shape are sensitive to R_{H5} at $W = 0.3$, whereas they appear almost independent of R_{H5} at $W = 2.0$. Moreover, a comparison between the spectra of panels A and B emphasizes the pronounced effects on the intensity, position, and width of the shoulder of the main peak determined by a W variation. Considering that the contributions to the CO band have been generally rationalized in terms of the two nonequivalent carbonyl groups of the surfactant differently located at the micellar core surface, the observed behavior can be attributed to the ability of water to screen the CO/Yb(III) interaction while, at the lower W value, that of H5 to compete with CO as interacting species.[27]

The effects on the surfactant SO_3^- stretching band arising from changes of the water and H5 contents are presented in Figure 10. It can be noted that an appreciable position and shape change occurs at $W = 0.3$ by increasing R_{H5}, whereas the band is practically unchanged at $W = 2.0$. This finding clearly indicates that the SO_3^- groups are mainly located at the surface of the hydrophilic core and directly involved in interaction with Yb(III) at $W = 0.3$ while, at higher W, water is able to effectively screen this interaction. The overall picture arising from the IR spectra analysis is that water is able to preferentially solvate Yb(III), SO_3^-, and CO so that only at very low water content these moieties may either interact with each other or with H5.

Further evidence on the H5/reversed micelles interactions are emphasized by the H5 CH and CN stretching bands occurring at about 3050 cm^{-1} and 1584 cm^{-1}, respectively.[28,29] These bands were obtained by subtracting the spectrum of the water/Yb(DEHSS)$_3$/*n*-heptane solution from that of H5/water/Yb(DEHSS)$_3$/*n*-heptane solution at the same W value. The com-

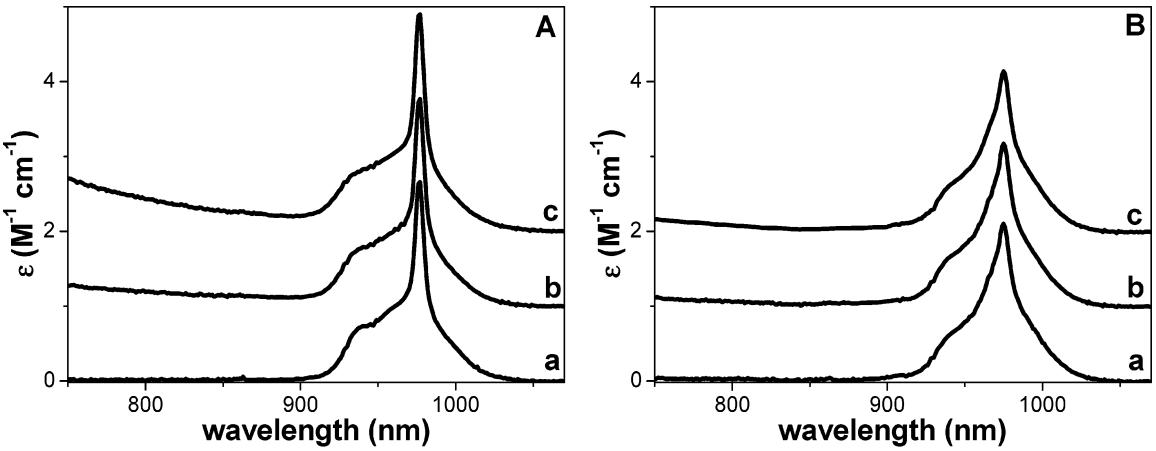

Figure 6. Absorption band of Yb(III) in H5/water/Yb(DEHSS)$_3$/*n*-heptane solutions at fixed surfactant concentration ([Yb(DEHSS)$_3$] = 0.020 M). Panel A: $W = 0.3$ and a, $R_{H5} = 0$; b, $R_{H5} = 0.73$; c, $R_{H5} = 1.52$. Panel B: $W = 2.0$ and a, $R_{H5} = 0$; b, $R_{H5} = 0.21$; c, $R_{H5} = 0.33$.

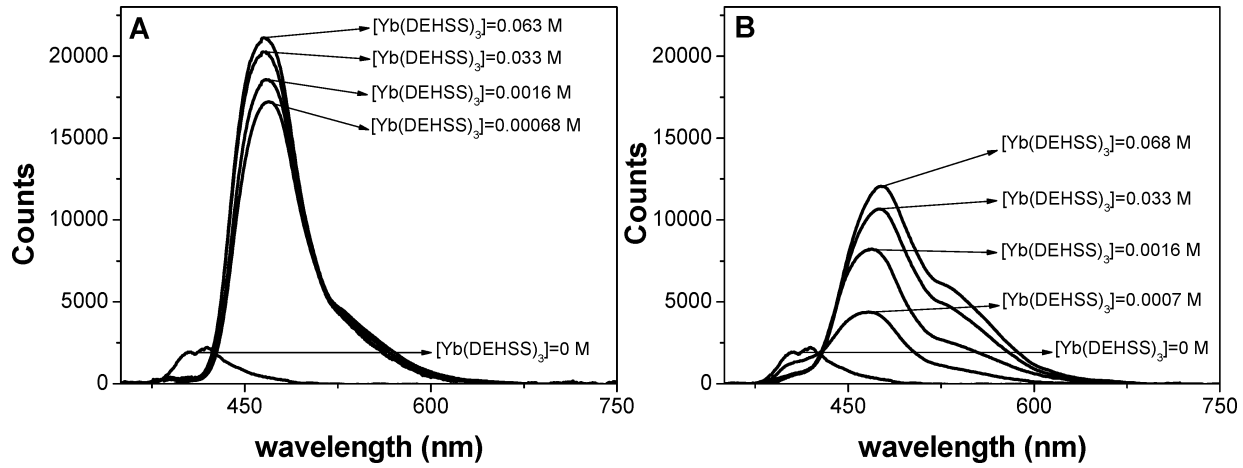

Figure 7. Photoluminescence spectra of H5/water/Yb(DEHSS)$_3$/*n*-heptane solutions at various surfactant concentrations and fixed H5 concentration ([H5] = 1.23×10^{-4} M). Panel A, $W = 0.6$; panel B, $W = 2.0$.

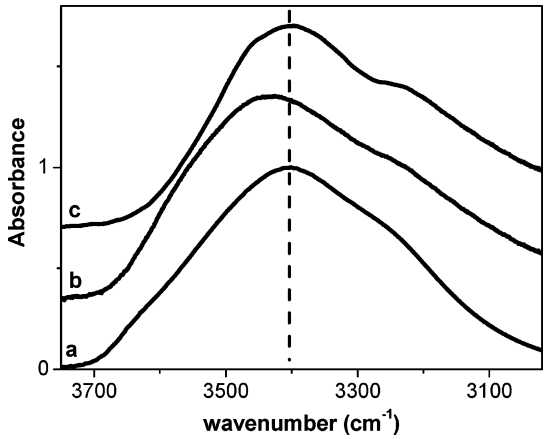

Figure 8. Water OH stretching band in (a) pure H_2O and water/Yb(DEHSS)$_3$/*n*-heptane solutions at (b) $W = 2.0$ and (c) $W = 0.3$. ([Yb(DEHSS)$_3$] = 0.020 M).

parison of these bands of H5 in *n*-heptane solution with those in H5/water/Yb(DEHSS)$_3$/*n*-heptane solutions is presented in Figures 11 and 12, respectively. To make these comparisons feasible, the bands were normalized to the same height of the peaks at about 3054 cm^{-1} and 1600 cm^{-1}, respectively. It can be noted that the bands relative to the H5/water/Yb(DEHSS)$_3$/*n*-heptane solutions are different from those of the H5/*n*-heptane solution. This behavior is more marked at the lower *W* value. Moreover, at $W = 0.3$, additional bands at about 3073, 3148, 3240, and 3280 cm^{-1} appear which are absent in the spectrum of H5/*n*-heptane solution. At the same time, the more intense peak occurring at 1601 cm^{-1} observed in H5/*n*-heptane solution disappears in the micellar solutions. All these findings emphasize the occurrence of some changes in the vibrational dynamics of H5, and they can be taken as further clues that H5 is confined in reversed micelles. Since the samples at $W = 0.3$ show changes stronger than that at $W = 2.0$, it can be also argued that the water content influences significantly the location of H5 within the reversed micelles.

Further understanding of the phenomena underlying the FT-IR spectra of Figures 11 and 12 may be gathered from DFT-B3LYP/6-31g** calculations of vibrational absorption spectra of the H5 molecule in vacuo. The two portions of the spectra relative to the regions 2900−3400 cm^{-1} and 1500−1650 cm^{-1} are also reported in Figures 11 and 12, respectively. The spectra were calculated with the GAUSSIAN03 suite of programs[30] and were appropriately corrected for anharmonicity by shifting the results in frequency, differently for the two regions. The calculated spectra compare excellently with those of H5 in *n*-heptane solution. In the CH-stretching region, the band above 3000 cm^{-1} is well reproduced by our calculations, which additionally allow us to predict for H5 a band at ca. 2950 cm^{-1}, which corresponds to the local mode stretching of the CH bond closest to the N atom: in our experiment such a band is not observed, due to the overlapping CH stretching bands of *n*-heptane. From the assignment made on the basis of the calculated normal modes, one may attribute the observed couplet

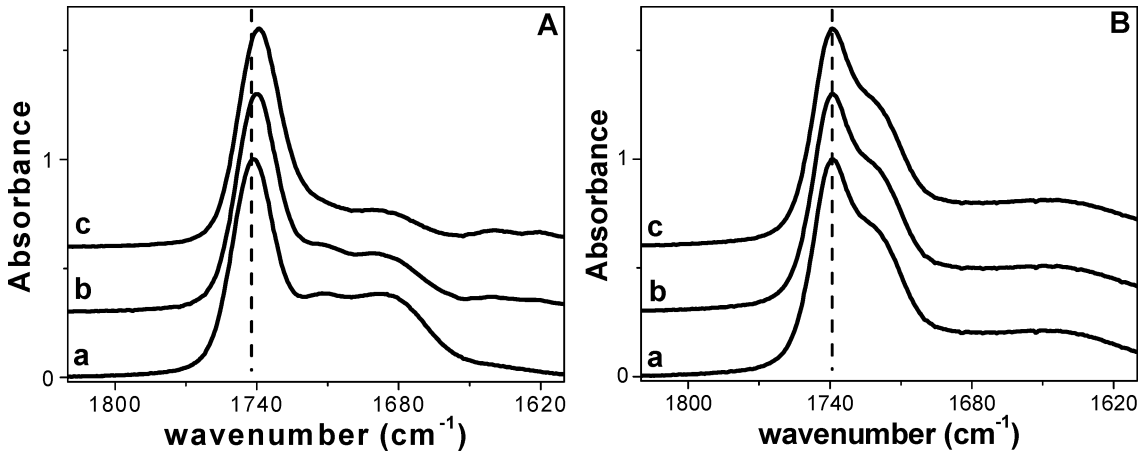

Figure 9. Surfactant CO stretching band in H5/water/Yb(DEHSS)$_3$/*n*-heptane solutions at fixed surfactant concentration ([Yb(DEHSS)$_3$] = 0.020 M). Panel A: $W = 0.3$ and a, $R_{H5} = 0$; b, $R_{H5} = 0.73$; c, $R_{H5} = 1.52$. Panel B: $W = 2.0$ and a, $R_{H5} = 0$; b, $R_{H5} = 0.21$; c, $R_{H5} = 0.33$.

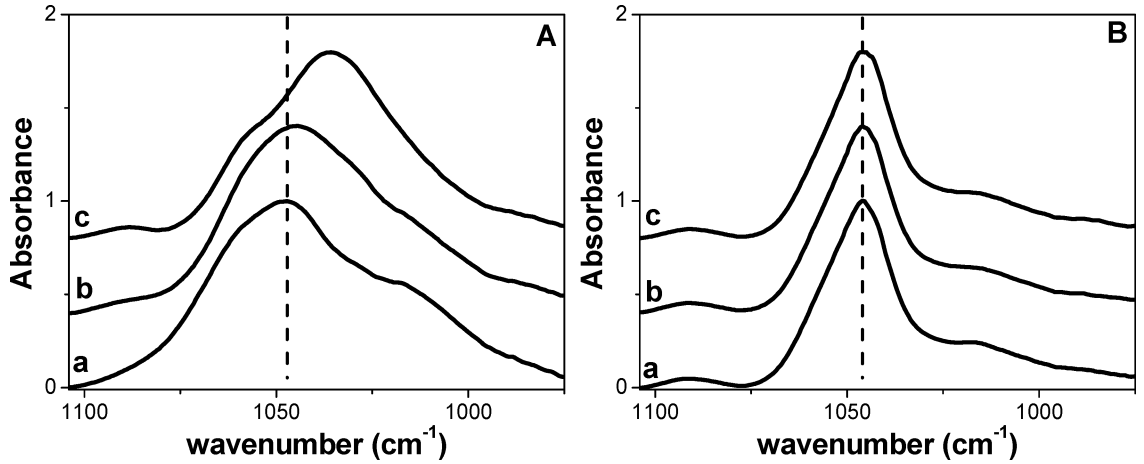

Figure 10. Surfactant SO_3^- stretching band in H5/water/Yb(DEHSS)$_3$/*n*-heptane solutions at fixed surfactant concentration ([Yb(DEHSS)$_3$] = 0.020 M). Panel A: $W = 0.3$ and a, $R_{H5} = 0$; b, $R_{H5} = 0.73$; c, $R_{H5} = 1.52$. Panel B: $W = 2.0$ and a, $R_{H5} = 0$; b, $R_{H5} = 0.21$; c, $R_{H5} = 0.33$.

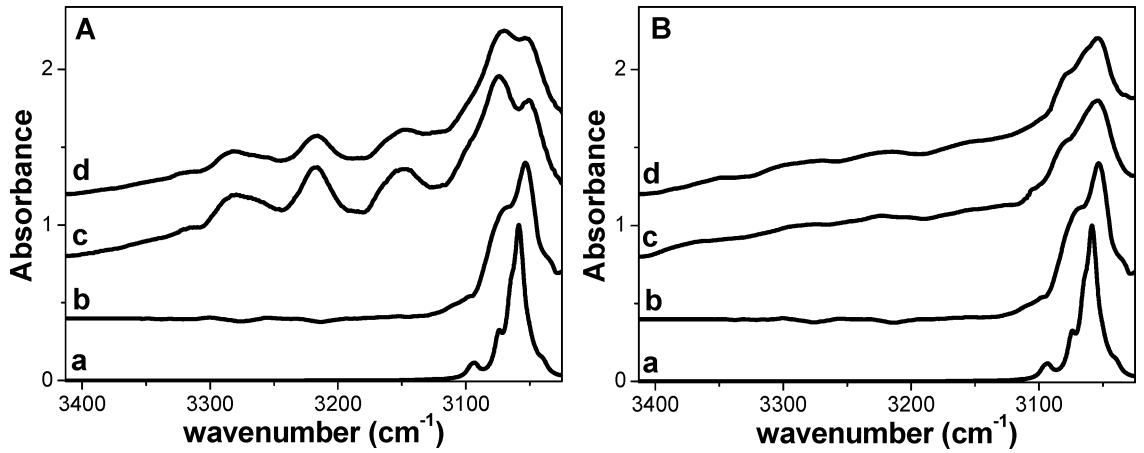

Figure 11. Comparison of the H5 CH stretching band in H5/*n*-heptane solution (spectrum b in both panels) with those in H5/water/Yb(DEHSS)$_3$/*n*-heptane solutions at fixed surfactant concentration ([Yb(DEHSS)$_3$] = 0.020 M). Panel A: $W = 0.3$ and c, $R_{H5} = 0.73$; d, $R_{H5} = 1.52$. Panel B: $W = 2.0$ and c, $R_{H5} = 0.21$; d, $R_{H5} = 0.33$. Spectrum a in both panels shows the calculated vibrational absorption bands of the H5 molecule in vacuo.

of bands at 1600 and 1585 cm^{-1} to normal modes with high content of CN stretching (the band at 1520 cm^{-1} is instead assigned to CC stretching ring deformation modes): such modes are expected to be highly perturbed by the presence of Yb(III), which most probably binds to the N atoms. Indeed in Figure 12 the two bands are observed to coalesce into a single band in presence of Yb(III), more so at $W = 0.3$ than at $W = 2.0$. In the latter case the binding of Yb(III) to H5 is strongly reduced by water.

SAXS Spectra. Typical X-ray scattering curves of H5/water/Yb(DEHSS)$_3$/*n*-heptane solutions are shown in Figure 13. The intensity rise observed in the presence of H5 indicates that the

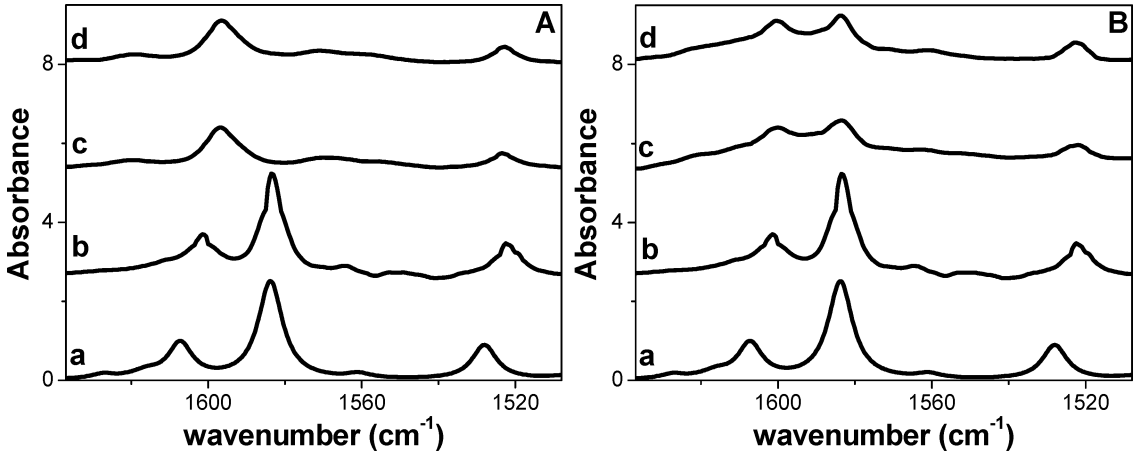

Figure 12. Comparison of the H5 CN stretching band in H5/*n*-heptane solution (spectrum b in both panels) with those in H5/water/Yb(DEHSS)$_3$/*n*-heptane solutions at fixed surfactant concentration ([Yb(DEHSS)$_3$] = 0.020 M). Panel A: $W = 0.3$ and c, $R_{H5} = 0.73$; d, $R_{H5} = 1.52$. Panel B: $W = 2.0$ and c, $R_{H5} = 0.21$; d, $R_{H5} = 0.33$. Spectrum a in both panels shows the calculated vibrational absorption bands of the H5 molecule in vacuo.

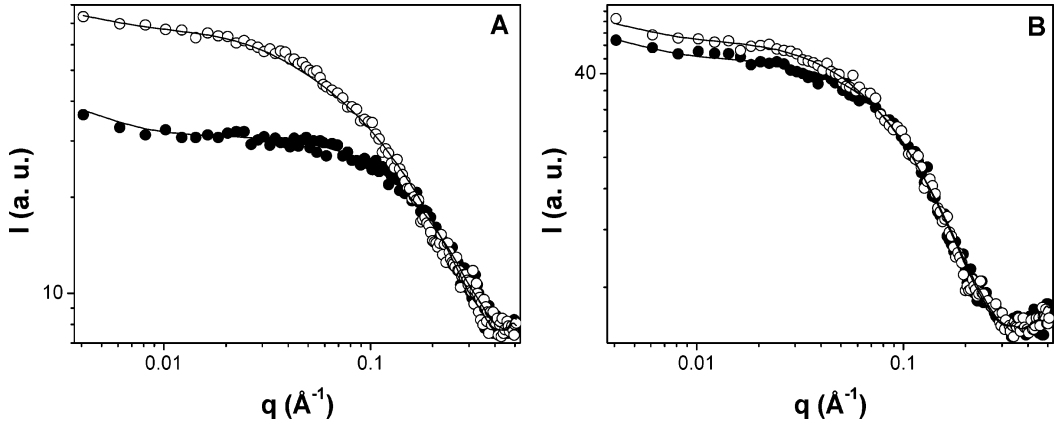

Figure 13. Typical smeared scattering profiles of H5/water/Yb(DEHSS)$_3$/*n*-heptane solutions at fixed surfactant concentration ([Yb(DEHSS)$_3$] = 0.020 M). Panel A: $W = 0.6$ and ●, $R_{H5} = 0$; ○, $R_{H5} = 1.32$. Panel B: $W = 2.0$ and ●, $R_{H5} = 0$; ○, $R_{H5} = 0.33$.

TABLE 1: Fitting Parameters Derived from the Least-Squares Analysis of the SAXS Data of the H5/Water/Yb(DEHSS)$_3$/*n*-Heptane System

		polydisperse sphere			monodisperse ellipsoid of rotation		
R_{H5}	W	r_m (Å)	b	χ^2	l_1 (Å)	l_2 (Å)	χ^2
0	0.6	7.8 ± 0.1	6.1 ± 0.1	0.14	7.8 ± 0.6	17 ± 3	0.13
0.73	0.6	9.0 ± 0.1	3.9 ± 0.1	0.70	7.9 ± 0.4	57 ± 10	0.16
1.32	0.6	9.4 ± 0.1	2.8 ± 0.1	1.57	9.2 ± 0.2	95 ± 11	0.31
0	2.0	10.7 ± 0.1	2.8 ± 0.1	0.26	13.3 ± 0.4	43 ± 7	0.20
0.21	2.0	10.7 ± 0.1	2.7 ± 0.1	0.36	12.6 ± 0.4	57 ± 10	0.16
0.33	2.0	10.9 ± 0.1	2.7 ± 0.1	0.37	12.8 ± 0.4	61 ± 10	0.20

aggregates become larger, consistent with the hypothesis that H5 is localized in the micellar aggregates.

Because X-ray scattering originates from the contrast between adjacent domains with different electron densities and the main discontinuity of the electron density occurs at the surfactant hydrophilic head group/hydrophobic alkyl chain interface, it must be stressed that the scattering centers must be identified with the hydrophilic cores of reversed micelles. Moreover, taking into account that the surfactant concentration was quite low ([Yb(DEHSS)$_3$] = 0.020 M), it can be plainly assumed that they behave as non-interacting particles. Then, to obtain information about the size and shape of these scattering centers and following a procedure elsewhere reported,[3] we compared the fittings of the experimental SAXS profiles using two models: polydisperse spheres and monodisperse ellipsoids of rotation. As a probe of the goodness of the fit we used the parameter χ^2, calculated by

$$\chi^2 = \frac{1}{N_{pt} - N_{par}} \sum_{i=1}^{N_{pt}} \frac{(I_{i,fit} - I_{i,exp})^2}{\sigma_i} \qquad (2)$$

where each $I_{i,fit}$ is the calculated scattering intensity, $I_{i,exp}$ is the experimental scattering intensity, σ_i is the variance ($\sigma_i = \sqrt{I_{i,exp}}$), and the summation runs over all the N_{pt} experimental points. The fitting results, the mean radius r_m, and the size distribution parameter b for the polydisperse spheres and the semiaxes l_1 and l_2 for the monodisperse ellipsoids together with the relative χ^2 are reported in Table 1. As a general consideration, all SAXS spectra were found to be well-fitted by both models. However, it can be noted that at $R_{H5} = 0$ the model of monodisperse

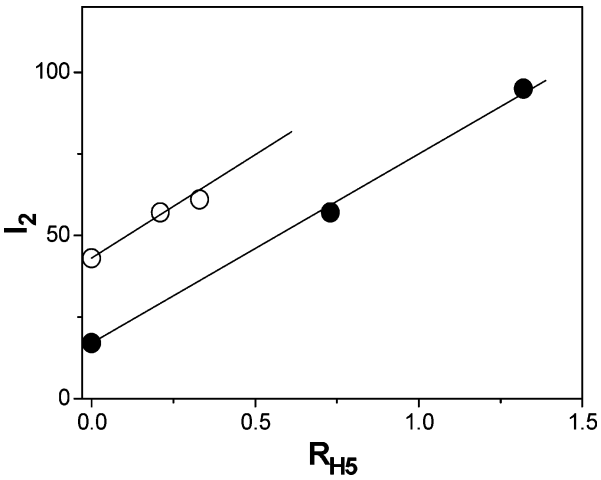

Figure 14. Plots of the semi axis l_2 as a function of R_{H5} at $W = 0.6$ (●) and $W = 2.0$ (○).

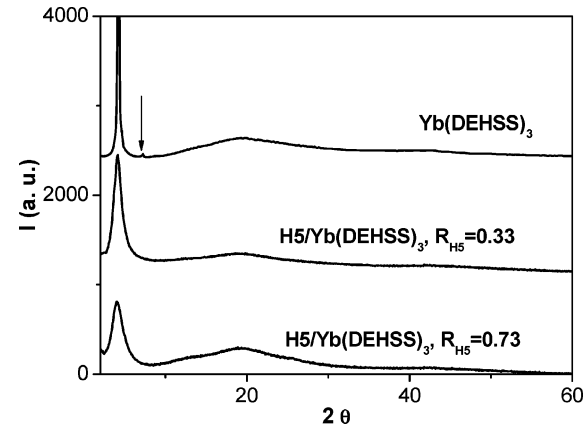

Figure 15. X-ray powder diffraction patterns of pure $Yb(DEHSS)_3$ and $H5/Yb(DEHSS)_3$ composites at the R_{H5} shown.

ellipsoids gives χ^2 values comparable with those of polydisperse spheres so that it is not feasible to establish unequivocally the aggregate shape. On the other hand, at $R_{H5} > 0$, the model of monodisperse ellipsoids gives χ^2 values lower than those of polydisperse spheres suggesting that at least in the presence of H5 the micelles are elongated and nearly monodisperse. Moreover, an inspection of Table 1 as well as of Figure 14 emphasizes that by increasing the H5 content there is a quite linear unidimensional growth of the reversed micelles suggesting that H5 is preferentially solubilized, opportunely oriented, in the micellar palisade layer without forming an internal core. The stabilization of longer aggregates due to increasing amounts of H5 as well as of water can be attributed to the screening effect of Yb^{3+}/Yb^{3+} and surfactant head group/head group repulsions arising from their insertion in the hydrophilic micellar nanodomain.

WAXS Spectra. Interesting H5/surfactant solid composites were obtained simply evaporating under vacuum the solutions of H5-containing $Yb(DEHSS)_3$ reversed micelles. X-ray powder diffraction spectra of these $H5/Yb(DEHSS)_3$ composites at various R_{H5} are shown in Figure 15. It can be noted that all the spectra are characterized by a quite intense peak at low 2θ values and a broad peak, due to the amorphous domain formed by the surfactant tails, at about $2\theta = 19°$.[31]

The position of the peaks of pure $Yb(DEHSS)_3$ occurring at $2\theta = 4.25°$ and 7.25°, converted in interplanar distances by the Bragg equation, were found to be in the ratio $1:1/\sqrt{3}$ (see Table 2). This involves that pure $Yb(DEHSS)_3$ forms liquid crystals

TABLE 2: Peak Position and Lattice Parameters of Pure and H5 Containing $Yb(DEHSS)_3$ Liquid Crystals

R_{H5}	2θ	d_{100} (Å)	2θ	d_{110} (Å)
0	4.25	20.8	7.25	12.2
0.33	4.13	21.4	–	–
0.73	4.03	21.9	–	–

characterized by a two-dimensional hexagonal structure.[31] On the other hand, in addition to the main peak, no secondary peaks were found in the composite spectra. For this reason we were unable to establish whether or not the bidimensional hexagonal structure is retained in the presence of H5. It can be also observed that, by increasing R_{H5}, the intensity of the main peak decreases while its width increases implying that the addition of H5 causes a greater structural disorder in the liquid crystalline phase and/or a decrease of the mean length of the surfactant rods.[32] In addition, a perusal of the lattice parameters of Table 2 indicates that, by increasing R_{H5}, only a slight increase of the d_{100} distance occurs involving that H5 is entrapped in the palisade layer formed by the oriented surfactant molecules. Finally, it is worth to note the absence in the spectra of $H5/Yb(DEHSS)_3$ composites of the diffraction peaks of pure solid H5 assuring that it is dispersed in the surfactant liquid crystals molecularly or in a quite disordered state.[15]

Conclusions

Interesting information concerning the binding strength, photophysical properties, and structural effects of 5-aza[5]-helicene (H5) in solutions of ytterbium bis(2-ethylhexyl) sulfosuccinate ($Yb(DEHSS)_3$) reversed micelles were achieved through the synergic use of several physicochemical techniques. The results suggest that H5 is practically totally confined in the reversed micelles at $W = 0.6$ whereas it is partitioned between the bulk organic phase and the reversed micelles at $W = 2.0$ and that consequently the binding of H5 to reversed micelles as well as its preferential solubilization site depend critically on the water to surfactant molar ratio. It has been also found that the driving force of the H5 binding is mainly its interaction with the Yb(III) surfactant counterion and the incorporation of increasing amounts of H5 involves a structural rearrangement of reversed micelles leading to a linear unidimensional growth of monodisperse ellipsoidal micellar aggregates. In such conditions, it can be speculated that the confined H5 could behave as an active laser medium entrapped in a resonating type nanocavity. Finally, from an analysis of WAXS spectra, it has been found that H5 is inserted within $Yb(DEHSS)_3$ liquid crystals molecularly or in a quite amorphous state while the entrapment of finite amounts of H5 causes marked increase of the structural disorder of the $Yb(DEHSS)_3$ liquid crystals.

Acknowledgment. The authors thank University of Palermo (Università di Palermo, Fondi Ricerca Scientifica ex 60%) and MIUR (PRIN2004) for financial support and Prof. Giovanna Longhi, University of Brescia, for help in the calculations of absorption IR spectra of H5.

References and Notes

(1) Calandra, P.; Giordano, C.; Ruggirello, A.; Turco Liveri, V. *J. Colloid Interface Sci.* **2004**, *277*, 206.

(2) Calandra, P.; Longo, A.; Marcianò, V.; Turco Liveri, V. *J. Phys. Chem. B* **2003**, *107*, 6724.

(3) Calandra, P.; Longo, A.; Ruggirello, A.; Turco Liveri, V. *J. Phys. Chem. B* **2004**, *108*, 8260.

(4) Mwalupindi, A. G.; Blyshak, L. A.; Ndou, T. T.; Warner, I. M. *Anal. Chem.* **1991**, *63*, 1326.

(5) Mwalupindi, A. G.; Ndou, T. T.; Warner, I. M. *Anal. Chem.* **1992**, *64*, 1840.
(6) Eastoe, J.; Towey, T. F.; Robinson, B. H.; Williams, J.; Heenan, R. H. *J. Phys. Chem.* **1993**, *97*, 1459.
(7) Eastoe, J.; Steytler, D. C.; Robinson, B. H.; Heenan, R. H.; North, A. N.; Dore, J. C. *J. Chem. Soc. Faraday Trans. I* **1994**, *90*, 2479.
(8) Turco Liveri, V. In *Nanosurface Chemistry, Vol. 1*; Rosoff M., Ed.; Dekker: New York, 2001; pp 473−504.
(9) Verbiest, T.; Van Elshocht, S.; Kauranen, M.; Hellemans, L.; Snauwaert, J.; Nuckolls, C.; Katz, T. J.; Persoons, A. *Science* **1998**, *282*, 913.
(10) Philips, K. E. S.; Katz, T. J.; Jockusch, S.; Lovinger, A.; Turro, N. J. *J. Am. Chem. Soc.* **2001**, *123*, 899.
(11) Grell, M.; Bradley, D. G. *Adv. Mater.* **1999**, *11*, 895.
(12) Oda, M.; Meskers, S. C. J.; Nothofer, H. G.; Scherf, U.; Nehrer, D. *Synth. Met.* **2000**, *111*−*112*, 575.
(13) Lightner, D. A.; Hefelfinger, D. T.; Powers, T. W.; Frank, G. W.; Trueblood, K. N. *J. Am. Chem. Soc.* **1971**, *93*, 2968.
(14) Martin, R. H. *Angew. Chem. Intl. Ed.* **1974**, *13*, 649.
(15) Bazzini, C.; Brovelli, S.; Caronna, T.; Gambarotti, C.; Giannone, M.; Macchi, P.; Meinardi, F.; Mele, A.; Panzeri, W.; Recupero, F.; Sironi, A.; Tubino, R. *Eur. J. Org. Chem.* **2005**, *7*, 1247.
(16) Bonner, O. D.; Choi, Y. S. *J. Phys. Chem.* **1974**, *78*, 1723.
(17) Calvaruso, G.; Minore, A.; Turco Liveri, V. *J. Colloid Interface Sci.* **2001**, *243*, 227.
(18) Giordano, C.; Longo, A.; Ruggirello, A.; Turco Liveri, V.; Venezia, A. M. *Colloid Polym. Sci.* **2004**, *283*, 265.
(19) Lebon, F.; Longhi, G.; Gangemi, F.; Abbate, S.; Priess, J.; Juza, M.; Bazzini, C.; Caronna, T.; Mele, A. *J. Phys. Chem. A* **2004**, *108*, 11752.
(20) Lei, G.; Anderson, J. E.; Buchwald, M. I.; Edwards, B. C.; Epstein, R. I. *Phys. Rev. B* **1998**, *57*, 7673.
(21) Di Bari, L.; Lelli, M.; Pintacuda, G.; Piscitelli, G.; Marchetti, F.; Salvadori, P. *J. Am. Chem. Soc.* **2003**, *125*, 5549.
(22) Onori, G.; Santucci, A. *J. Phys. Chem.* **1993**, *97*, 5430.
(23) Giordano, C.; Longo, A.; Turco Liveri, V.; Venezia, A. M. *Colloid Polym. Sci.* **2003**, *281*, 229.
(24) Ceraulo, L.; Filizzola, F.; Longo, A.; Ruggirello, A.; Turco Liveri, V. *Colloid Polym. Sci.* **2006**, *284*, 1085.
(25) Horrocks, W. D., Jr.; Bolender, J. P.; Smith, W. D.; Supkowski, R. *J. Am. Chem. Soc.* **1997**, *119*, 5972.
(26) Li, Q.; Weng, S.; Wu, J.; Zhou, N. *J. Phys. Chem. B* **1998**, *102*, 3168.
(27) Calandra, P.; Caponetti, E.; Chillura Martino, D.; D'Angelo, P. D.; Minore, A.; Turco Liveri, V. *J. Mol. Struct.* **2000**, *522*, 165.
(28) Haq, S.; King, D. A. *J. Phys. Chem.* **1996**, *100*, 16957.
(29) Dobrowolski, J. C. *J. Mol. Struct.* **2003**, *651*, 607.
(30) Frisch, M. J.; Trucks, G. W.; Schlegel, H. B.; Scuseria, G. E.; Robb, M. A.; Cheeseman, J. R.; Montgomery, J. A., Jr.; Vreven, T.; Kudin, K. N.; Burant, J. C.; Millam, J. M.; Iyengar, S. S.; Tomasi, J.; Barone, V.; Mennucci, B.; Cossi, M.; Scalmani, G.; Rega, N.; Petersson, G. A.; Nakatsuji, H.; Hada, M.; Ehara, M.; Toyota, K.; Fukuda, R.; Hasegawa, J.; Ishida, M.; Nakajima, T.; Honda, Y.; Kitao, O.; Nakai, H.; Klene, M.; Li, X.; Knox, J. E.; Hratchian, H. P.; Cross, J. B.; Adamo, C.; Jaramillo, J.; Gomperts, R.; Stratmann, R. E.; Yazyev, O.; Austin, A. J.; Cammi, R.; Pomelli, C.; Ochterski, J. W.; Ayala, P. Y.; Morokuma, K.; Voth, G. A.; Salvador, P.; Dannenberg, J. J.; Zakrzewski, V. G.; Dapprich, S.; Daniels, A. D.; Strain, M. C.; Farkas, O.; Malick, D. K.; Rabuck, A. D.; Raghavachari, K.; Foresman, J. B.; Ortiz, J. V.; Cui, Q.; Baboul, A. G.; Clifford, S.; Cioslowski, J.; Stefanov, B. B.; Liu, G.; Liashenko, A.; Piskorz, P.; Komaromi, I.; Martin, R. L.; Fox, D. J.; Keith, T.; Al-Laham, M. A.; Peng, C. Y.; Nanayakkara, A.; Challacombe, M.; Gill, P. M. W.; Johnson, B.; Chen, W.; Wong, M. W.; Gonzalez, C.; Pople, J. A. *Gaussian 03, Revision B.05*; Gaussian, Inc.: Pittsburgh, PA, 2003.
(31) Ekwall, P.; Mandell, L.; Fontell, K. *J. Colloid Interface Sci.* **1970**, *33*, 215.
(32) Kumar, A.; Kuneida, H.; Vazquez, C.; Lopez-Quintela, M. A. *Langmuir* **2001**, *17*, 7245.